

# Baryon flow from SIS to AGS energies

P. K. Sahu<sup>1\*</sup>, W. Cassing<sup>2</sup>, U. Mosel<sup>2</sup> and A. Ohnishi<sup>1</sup>

<sup>1</sup> *Division of Physics, Graduate School of Science, Hokkaido University, Sapporo 060-0810, Japan*

<sup>2</sup> *Institut für Theoretische Physik, Universität Giessen, D-35392 Giessen, Germany*

## Abstract

We analyze the baryon sideward and elliptic flow from SIS (0.25 ~ 2 AGeV) to AGS (2 ~ 11.0 AGeV) energies for Au + Au collisions in the relativistic transport model RBUU that includes all baryon resonances up to a mass of 2 GeV as well as string degrees of freedom for the higher mass continuum. There are two factors which dominantly determine the baryon flow at these energies: the momentum dependence of the scalar and vector potentials and the resonance-string degrees of freedom. We fix the explicit momentum dependence of the nucleon-meson couplings within the NL3 parameter set by the nucleon optical potential up to 1 GeV of kinetic energy. When assuming the optical potential to vanish identically for  $E_{kin} \geq 3.5$  GeV we simultaneously reproduce the sideward flow data of the FOPI, EOS, E895 and E877 collaborations, the elliptic flow data of the EOS, E895 and E877 collaborations, and approximately the rapidity and transverse mass distribution of protons at AGS energies. The gradual change from hadronic to string degrees of freedom with increasing bombarding energy can be viewed as a transition from *hadronic* to *string* matter, i.e. a dissolution of hadrons.

PACS: 25.75.-q, 24.10.Jv, 25.75.Ld

Keywords: Relativistic heavy-ion collisions, Relativistic models, Collective flow

arXiv:nucl-th/9907002v2 24 Nov 1999

---

\*JSPS Research Fellow.

## I. INTRODUCTION

The nuclear equation of state (EoS) plays a central role in heavy-ion collisions [1] – [11] as well as for the maximum mass of neutron stars and supernova explosions. Therefore, the nuclear EoS is one of the most challenging topics in nuclear physics, i.e. to understand the nature of the nuclear force at high density and/or temperature. In nucleus-nucleus collisions the transverse flow observables, including directed [8] and elliptic flow [10,11], as well as subthreshold particle production [12] are sensitive to the nuclear EoS. Recently, both the directed transverse flow (sideward flow) and the flow tensor (elliptic flow) have been measured and reported in Refs. [7] – [9], [13] – [17] for heavy-ion (Au + Au) collisions in the incident energy range of  $1A \text{ GeV} \leq E_{inc} \leq 11A \text{ GeV}$ . In this energy range the directed transverse flow first grows, saturates at around  $2A \text{ GeV}$  and then decreases experimentally with energy showing no minimum as expected from hydrodynamical calculations including a first order phase transition in the EoS [18]. On the other hand the elliptic flow measured experimentally changes its sign from negative (squeeze-out) to positive (in-plane) as a function of incident energy in the range of  $1A \text{ GeV} \leq E_{inc} \leq 11A \text{ GeV}$ .

In this work we analyze the directed transverse flow in the incident energy range starting from GSI-SIS to the BNL-AGS regime by using the relativistic transport model RBUU which includes the two essential ingredients, i.e. i) the momentum-dependent potentials and ii) the resonance/string degrees of freedom. With these ingredients fixed we examine the sideward and the elliptic flow of protons as a function of the incident energy up to AGS energies of  $\sim 1 - 11A \text{ GeV}$ .

We recall that relativistic transport models have been extensively used to describe the heavy-ion data at energies starting from the SIS at GSI to the SPS regime at CERN, [1,10,19–23]. Among them the Relativistic Boltzmann-Uehling-Uhlenbeck (RBUU) approach is one of the most successful models. It incorporates the relativistic mean-field (RMF) theory, which is applicable to various nuclear structure problems as well as for neutron star studies [24]. Thus it is possible to refine the mean-field part of RBUU by incorporating constraints from the latter fields. Here we base our study on the NL3 parameter set from Ref. [25] since this parameter set has been widely applied in the analysis of heavy-ion collisions [26–28].

The most simple versions of RMF theories assume that the scalar and vector fields are represented by point-like meson-baryon couplings. These couplings lead to a linearly growing Schrödinger-equivalent potential in nuclear matter as a function of the kinetic energy  $E_{kin}$ , which naturally explains the energy dependence of the nucleon optical potential at low energies ( $\leq 200 \text{ MeV}$ ). However, a simple RMF does not describe the nucleon optical potential at higher energies, where the optical potential deviates substantially from a linear function and saturates at  $E_{kin} \approx 1 \text{ GeV}$ . Since the energy dependence of sideward flow is controlled in part by the nucleon optical potential, the simple RMF cannot be applied to high-energy heavy-ion collision problems. In order to remedy this aspect, some RBUU approaches invoke an explicit momentum dependence of the coupling constant, i.e. a form factor for the meson-baryon couplings [1,21].

In our earlier work on directed flow in nucleus-nucleus collisions [26] we showed that the scalar and vector self energies for nucleons including a momentum and density dependence are the key quantities which determine the behaviour of flow at SIS energies and explain the kinetic energy dependence of the nucleon optical potential as well. In this study we proceed with the systematic analysis of flow up to AGS energies using the latter explicitly momentum-dependent relativistic mean fields.

A further important ingredient at AGS energies are the resonance/string degrees of freedom which are excited during the reaction in high energy baryon-baryon or meson-baryon collisions. While at SIS energies particle production mainly occurs through baryon

resonance production and their decay, the string phenomenology is found to work well at SPS energies [1]. We note here that both mechanisms really describe the same physics, i.e. the decay of excited baryons or mesons. The only essential difference is the treatment of the decay of these excited states: while the baryon resonances all decay to  $N + \text{meson}$  (or  $N^* + \text{meson}$ ) the strings can decay to  $Nn\pi$  ( $n > 1$ ). Due to these different decay schemes there are various ways to implement elementary cross sections in transport models [1,10,27–30]. One of the extremes is to parameterize all possible cross sections for multi-pion production,  $NN \rightarrow NNn\pi$  ( $n \geq 3$ ) only through  $N, \Delta, \pi$  degrees of freedom; the other extreme is to fully apply string phenomenology in this energy region without employing any resonances. Although it is possible to reproduce the elementary cross sections from  $NN$  and  $\pi N$  collisions and the inclusive final hadron spectra in heavy-ion collisions within these different models, we expect that differences should appear in the dynamical evolution of the system, e.g. in the thermodynamical properties [30,31] and in collective flow [30]. For example, if thermal equilibrium is achieved at a given energy density, models with a larger number of degrees of freedom including strings will give smaller temperature and pressure. Since the transverse flow is partly made up from this pressure, we expect a reduction of flow for models with a larger number of degrees of freedom (strings) while a pure resonance gas including high mass baryon excitations may be of higher temperature and develop a larger pressure [32]. In order to investigate the sensitivity of observables to this point we introduce an energy scale  $\sqrt{s_{sw}}$  that separates the two production mechanisms.

We have employed here a new transport code that incorporates all nucleon resonances up to a mass of 2 GeV [33,34] and the Lund string model [35] for higher excitations as in the Hadron-String-Dynamics (HSD) approach [1,21]. In the practical implementation for  $NN$  or  $MN$  collisions at invariant energies lower (higher) than  $\sqrt{s_{sw}}$  resonances (strings) are assumed to be excited. In view of our basis space of baryon resonances up to 2 GeV the transition energy  $\sqrt{s_{sw}}$  has to be below 4 GeV. Since the transverse pressure from strings is smaller than that from resonances the transverse mass spectra of baryons should become softer for smaller  $\sqrt{s_{sw}}$ . As described below we fix this parameter by  $\sqrt{s_{sw}} \approx 3.5$  GeV in fitting the transverse mass spectra of protons in central Au + Au collisions at AGS energies.

We organize our work as follows: In Section 2 we briefly describe the relativistic transport approach with known constraints on the momentum dependence of the scalar and vector self energies. In Section 3 we will systematically study the transverse mass spectra for protons with and without momentum-dependent potentials as well as resonance/string degrees of freedom and compare the calculated sideward and elliptic flow with the experimental data. Section 4 concludes this study with a summary and discussion of open questions.

## II. THE RELATIVISTIC TRANSPORT MODEL

In the present calculation we perform a theoretical analysis along the line of the relativistic transport approach RBUU which is based on a coupled set of covariant transport equations for the phase-space distributions  $f_h(x, p)$  of a hadron  $h$  [1,21,36]. The model inputs are the nuclear mean fields and the (in-medium) elementary hadron-hadron cross sections. In the relativistic transport approach the nuclear mean field contains both vector- and scalar-potentials  $U^\nu$  and  $U^S$ , respectively, that depend on the nuclear density and momentum. In this work, these mean fields are calculated on the basis of the same Lagrangian density as considered in our earlier calculations [26], which contain nucleon,  $\sigma$  and  $\omega$  meson fields and nonlinear self-interactions of the scalar field (cf. NL3 parameter set [25]). The scalar and vector form factors at the vertices are taken into account in the form [21]

$$f_s(\mathbf{p}) = \frac{\Lambda_s^2 - \frac{1}{2}\mathbf{p}^2}{\Lambda_s^2 + \mathbf{p}^2} \quad \text{and} \quad f_v(\mathbf{p}) = \frac{\Lambda_v^2 - \frac{1}{6}\mathbf{p}^2}{\Lambda_v^2 + \mathbf{p}^2}, \quad (1)$$

where the cut-off parameters  $\Lambda_s = 1.0$  GeV and  $\Lambda_v = 0.9$  GeV are obtained by fitting the Schrödinger equivalent potential,

$$U_{sep}(E_{kin}) = U_s + U_0 + \frac{1}{2M}(U_s^2 - U_0^2) + \frac{U_0}{M}E_{kin}, \quad (2)$$

to Dirac phenomenology for intermediate energy proton-nucleus scattering [37]. The above momentum dependence is computed self-consistently on the mean-field level; in the actual calculations we evaluate  $U^0$  and  $U^S$  in the local rest frame of the surrounding nuclear matter and then perform a Lorentz transformation to get  $U^\mu$  in the calculation frame. Thus neglecting a nonlocality in time, this evaluation of the potential is practically covariant.

The resulting Schrödinger equivalent potential (2) at density  $\rho_0$  is shown in Fig. 1 as a function of the nucleon kinetic energy with respect to the nuclear matter at rest in comparison to the data from Hama et al. [37]. The increase of the Schrödinger equivalent potential up to  $E_{kin} = 1$  GeV is described quite well; then the potential decreases and is set to zero above 3.5 GeV.

For the transition rate in the collision term of the transport model we employ in-medium cross sections as in Ref. [33] that are parameterized in line with the corresponding experimental data for  $\sqrt{s} \leq \sqrt{s_{sw}}$ . For higher invariant collision energies we adopt the Lund string formation and fragmentation model [35] as incorporated in the HSD transport approach [1,21] which has been used extensively for the description of particle production in nucleus-nucleus collisions from SIS to SPS energies [1]. One might speculate that the transition rates change substantially with increasing baryon density. However, in this case the overall reproduction of baryon and pion rapidity distributions from SIS to SPS energies would be spoiled. In Ref. [1] no indication was found for the light quark sector whereas the enhanced production of strangeness at AGS energies (found experimentally) might be attributed to enhanced transition rates. Since this is presently an open question and discussed in a controversial manner, we discard the physics of strange hadrons in this work and concentrate on the collective aspects of nucleons and pions.

In the present relativistic transport approach (RBUU) as in our earlier work [26] we explicitly propagate nucleons and  $\Delta$ 's as well as all baryon resonances up to a mass of 2 GeV with their isospin degrees of freedom [33,34,38]. Furthermore,  $\pi, \eta, \rho, \omega, K, \bar{K}$  and  $\sigma$  mesons are propagated, too, where the  $\sigma$  is a short lived effective resonance that describes  $s$ -wave  $\pi\pi$  scattering. For more details we refer the reader to Refs. [33,38] concerning the low energy cross sections and to Refs. [1,21] with respect to the implementation of the string dynamics, respectively. We note that throughout this work we have neglected the momentum dependence of the potentials in the collision term in order to save computational time for the systematic analysis.

### III. COMPARISON TO EXPERIMENTAL DATA

#### A. Transverse mass spectra of protons

In Fig. 2 we show the proton transverse mass spectra (a) and rapidity distribution (b) in a central collision of Au + Au at 11.6 A GeV ( $b < 3.5$  fm) for  $\sqrt{s_{sw}} = 2.6$  GeV (dotted histograms) and 3.5 GeV (solid histograms) in comparison to the experimental data of the E802 collaboration [39]. A cascade calculation (crosses) is shown additionally for  $\sqrt{s_{sw}} = 3.5$  GeV to demonstrate the effect of the mean-field potentials which lead to a reduction of the transverse mass spectra below 0.3 GeV and a substantial hardening of the spectra. As expected, the transverse mass spectrum is softer for smaller  $\sqrt{s_{sw}}$  due to the larger number of degrees of freedom in the string model relative to the resonance model.

We note that strings may be regarded as hadronic excitations in the continuum of lifetime  $t_F \approx 0.8 \text{ fm}/c$  (in their rest frame) that take over a significant part of the incident collision energy by their invariant mass. They decay dominantly to light baryons and mesons and only to a low extent to heavy baryon resonances. Thus the number of particles for fixed system time is larger for string excitations than for the resonance model; in the former several hadrons propagate as a single heavy resonance which might be regarded as a cluster of a nucleon +  $n$  pions. As a consequence the translational energies are suppressed in string excitations and, as a result, the temperature as well as the pressure are smaller when exciting strings.

From the above comparison with the experimental transverse mass spectra for protons in Fig. 2 we fix  $\sqrt{s_{sw}} \approx 3.5 \text{ GeV}$ ; this implies that binary final baryon channels dominate in our transport model up to  $\sqrt{s} \approx 3.5 \text{ GeV}$  which corresponds to a proton laboratory energy  $T_{lab}$  of about 4.6 GeV. We mention that  $\sqrt{s_{sw}}$  may be changed by  $\pm 0.3 \text{ GeV}$  and still describe the proton spectra in Fig. 2.

## B. Directed flow for Au + Au collisions

We now turn to collective flow. The calculations are performed for the impact parameter  $b = 6 \text{ fm}$  for Au + Au systems, since for this impact parameter we get the maximum flow which corresponds to the multiplicity bins  $M3$  and  $M4$  as defined by the Plastic Ball collaboration [40] at BEVALAC/SIS energies. As in [26] we have calculated the flow

$$F = \left\langle \frac{d(P_x/A)}{dy} \right\rangle \Big|_{y=0} \quad (3)$$

by fitting a linear plus cubic term as a function of the normalized rapidity  $y = y_{cm}/y_{proj}$  for Au + Au systems at all energies.

In Fig. 3 the transverse flow (3) is displayed in comparison to the data from Refs. [7,9,13,16] as collected in Ref. [15] for Au + Au systems. The solid line (RBUU with  $\sqrt{s_{sw}} = 3.5 \text{ GeV}$ ) is obtained with the scalar and vector self energies as discussed above, i.e. Eq. (1). The dotted line (CASCADE with  $\sqrt{s_{sw}} = 3.5 \text{ GeV}$ ) corresponds to cascade calculations for reference in order to show the effect of the mean field relative to that from collisions. We observe that the solid line (RBUU, cf. Fig. 1) is in good agreement with the flow data at all energies; above bombarding energies of 6 A GeV the results are practically identical to the cascade calculations showing the potential effects to become negligible.

The sideward flow shows a maximum around 2 A GeV for Au + Au and decreases continuously at higher beam energy ( $\geq 2 \text{ A GeV}$ ) without showing any explicit minimum [18]. This is due to the fact that the repulsive force caused by the vector mean field decreases at high beam energies (cf. Fig. 1) such that in the initial phase of the collision there are no longer strong gradients of the potential within the reaction plane. In subsequent collisions, which are important for the Au + Au due to the system size, the kinetic energy of the particles relative to the local rest frame is then in a range ( $E_{kin} \leq 1 \text{ GeV}$ ) where the Schrödinger equivalent potential (at density  $\rho_0$ ) is determined by the experimental data [37].

We thus conclude that for the sideward flow data up to  $\leq 11 \text{ A GeV}$  one needs a considerably strong vector potential at low energy and that one has to reduce the vector mean field at high beam energy roughly in line with Fig. 1. In other words, there is only a weak repulsive force at high relative momenta and high densities.

Another aspect of the decreasing sideward flow can be related to the dynamical change in the resonance/string degrees of freedom as already discussed above. For instance, for  $\sqrt{s_{sw}} = 2.6 \text{ GeV}$  the calculated flow turns out to be smaller than the data above 1.5 A GeV and approaches the cascade limit already for  $\approx 3\text{-}4 \text{ A GeV}$ . This is due to the fact that in

strings the incident energy is stored to a larger extent in their masses and the translational energy is reduced accordingly. In addition – in the present treatment of string formation and decay – strings do not interact with other hadrons before their decay and thus do not contribute to pressure during this time. In this respect string-hadron or string-string interactions might become important when a sufficient part of hadrons are excited to strings during the heavy-ion reaction. We recall that the role of string fusion to create multi-strange (anti-)hyperons has already been pointed out in Refs. [28,41].

### C. Elliptic flow

Apart from the directed flow of protons, the elliptic flow provides additional information and constraints on the nuclear potentials involved [10]. In this respect the elliptic flow for protons [42]

$$v_2 = \left\langle \frac{(P_x^2 - P_y^2)}{(P_x^2 + P_y^2)} \right\rangle \quad (4)$$

for  $|y_{cm}/y_{proj}| \leq 0.2$  is shown in Fig. 4 as a function of the incident energy for Au + Au collisions at  $b = 6$  fm. The solid line (RBUU with  $\sqrt{s_{sw}} = 3.5$  GeV) is obtained with the same mean fields as in Fig. 3 while the dotted line (CASCADE with  $\sqrt{s_{sw}} = 3.5$  GeV) stands again for the cascade results. The flow parameter  $v_2$  changes its sign from negative at low energies ( $\leq 5A$  GeV) to positive elliptic flow at high energies ( $\geq 5A$  GeV). We observe that the solid line is in good agreement with data, where the data points are from the EOS [9], E895 [16] and E877 [13] collaborations and taken from Ref. [17].

This can be understood as follows: At low energies the squeeze-out of nuclear matter leads to a negative elliptic flow since projectile and target spectators distort the collective expansion of the 'fireball' in the reaction plane. At high energies the projectile and target spectators do not hinder anymore the in-plane expansion of the 'fireball' due to their high velocity ( $\approx c$ ); the elliptic flow then is positive. The competition between squeeze-out and in-plane elliptic flow at AGS energies depends on the nature of the nuclear force as pointed out already by Danielewicz et al. [10]. We note, however, that in our calculation with the momentum-dependent potential (Fig. 1) we can describe both the sideward as well as elliptic flow data [7–9,13–17] simultaneously.

In our cascade calculation (Fig. 4) the elliptic flow from squeeze-out is weaker due to the lack of a nuclear force; this demonstrates the relative role of the momentum-dependent nuclear potentials on the  $v_2$  observable below bombarding energies of about 5 A GeV.

## IV. SUMMARY

In this work we have calculated the baryon sideward and elliptic flow in the energy range up to 11 A GeV in the relativistic transport model RBUU for Au + Au collisions. We found that in order to reach a consistent understanding of the nucleon optical potential up to 1 GeV, the transverse mass distributions of protons at AGS energies as well as the excitation function of sideward and elliptic flow [7–9,13–17] up to 11 A GeV, the strength of the vector potential has to be reduced in the RBUU model at high relative momenta and/or densities. Otherwise, too much flow is generated in the early stages of the reaction and cannot be reduced at later phases where the Schrödinger equivalent potential is experimentally known. This constrains the parameterizations of the explicit momentum dependence of the vector and scalar mean fields  $U^\nu$  and  $U^S$  in Eq. (1) at high momenta where no data for elastic  $pA$  scattering are available.

In addition, we have shown the relative role of resonance and string degrees of freedom at AGS energies. By reducing the number of degrees of freedom via high mass resonances one can build up a higher pressure and/or temperature of the 'fireball' which shows up in the transverse mass spectra of protons as well as in the sideward flow [30]. A possible transition from resonance to string degrees of freedom is indicated by our calculations at invariant baryon-baryon collision energies of  $\sqrt{s} \approx 3.5 \pm 0.3$  GeV which corresponds to a proton laboratory energy of about 3.6 – 5.8 GeV. Due to Fermi motion of the nucleons in Au + Au collisions the transition from resonance to string degrees of freedom becomes smooth and starts from about 3 A GeV; at 11 A GeV practically all initial baryon-baryon collisions end up in strings, i.e. hadronic excitations in the continuum that decay to hadrons on a time scale of about 0.8 fm/c in their rest frame. This initial high-density *string matter* (up to  $10 \rho_0$  at 11 A GeV) should not be interpreted as *hadronic matter* since it implies roughly 5 constituent quarks per fm<sup>3</sup>, which is more than the average quark density in a nucleon.

The authors are grateful to D. Keane for valuable comments on the experimental data sets. One of us (PKS) likes to acknowledge the support from the JSPS, Japan. This work was also supported by GSI Darmstadt.

## REFERENCES

- [1] W. Cassing and E. L. Bratkovskaya, Phys. Rep. **308** (1999) 65.
- [2] H. Stöcker and W. Greiner, Phys. Rep. **137** (1986) 277.
- [3] H. H. Gutbrod, A. M. Poskanzer and H. G. Ritter, Rep. Prog. Phys. **52** (1989) 1267.
- [4] C. Gale, G. M. Welke, M. Prakash, S. J. Lee, and S. Das Gupta, Phys. Rev. **C 41** (1990) 1545.
- [5] J. Zhang, S. Das Gupta and C. Gale, Phys. Rev. **C 50** (1994) 1617.
- [6] M. D. Partlan et al., Phys. Rev. Lett. **75** (1995) 2100.
- [7] N. Herrmann et al., Nucl. Phys. **A 610** (1996) 49c.
- [8] W. Reisdorf and H. G. Ritter, Ann. Rev. Nucl. Part. Sci. **47** (1997) 1.
- [9] J. Chance et al., Phys. Rev. Lett. **78** (1997) 2535.
- [10] P. Danielewicz et al., Phys. Rev. Lett. **81** (1998) 2438; P. Danielewicz, nucl-th/9902043.
- [11] J. -Y. Ollitrault, Phys. Rev. D **46** (1992) 229; H. Sorge, Phys. Rev. Lett. **78** (1997) 2309.
- [12] W. Cassing, V. Metag, U. Mosel, and K. Niita, Phys. Rep. **188** (1990) 363; W. Cassing and U. Mosel, Prog. Part. Nucl. Phys. **25** (1990) 235.
- [13] J. Barrette et al., Phys. Rev. C **56** (1997) 3254.
- [14] P. Braun-Munzinger and J. Stachel, Nucl. Phys. **A 638** (1998) 3c.
- [15] H. Liu et al., Nucl. Phys. **A 638** (1998) 451c.
- [16] P. Chung et al., J. Phys. G **25** (1999) 255.
- [17] C. Pinkenburg et al., Phys. Rev. Lett. **83** (1999) 1295.
- [18] D. Rischke, Nucl. Phys. **A 610** (1996) 88c.
- [19] Q. Pan and P. Danielewicz, Phys. Rev. Lett. **70** (1993) 2062.
- [20] T. Maruyama, W. Cassing, U. Mosel, S. Teis and K. Weber, Nucl. Phys. **A 573** (1994) 653.
- [21] W. Eehalt and W. Cassing, Nucl. Phys. **A 602** (1996) 449; J. Geiss, W. Cassing and C. Greiner, Nucl. Phys. **A 644** (1998) 107.
- [22] S.A. Bass et al., Prog. Part. Nucl. Phys. **41** (1998) 225 ; J. Phys. **G 25** (1999) R1.
- [23] G. Q. Li, G. E. Brown, C. H. Lee and C. M. Ko, nucl-th/9702023 (1997); nucl-th/9703040 (1997).
- [24] S. K. Ghosh, S. C. Phatak and P. K. Sahu, Z. Phys. **A352** (1996) 457.
- [25] A. Lang, B. Blättel, W. Cassing, V. Koch, U. Mosel and K. Weber, Z. Phys. **A 340** (1991) 207.
- [26] P. K. Sahu, A. Hombach, W. Cassing, M. Effenberger and U. Mosel, Nucl. Phys. **A 640** (1998) 493, and references therein.
- [27] B. A. Li, C. M. Ko, A. T. Sustich, and B. Zhang, Phys. Rev. **C 60** (1999) 011901.
- [28] S. Soff et al., nucl-th/9903061.
- [29] Y. Nara, N. Otuka, A. Ohnishi, K. Niita and S. Chiba, nucl-th/9904059.
- [30] A. Hombach, W. Cassing, S. Teis and U. Mosel, Eur. Phys. J. **A5** (1999) 157.
- [31] Y. Nara, N. Otuka, A. Ohnishi and T. Maruyama, Prog. Theor. Phys. Suppl. **129** (1997) 33.
- [32] M. Belkacem, M. Brandstetter, S. A. Bass et al., Phys. Rev. **C 58** (1998) 1727; L. V. Bravina et al., J. Phys. **G 25** (1999) 351.
- [33] M. Effenberger, E. L. Bratkovskaya and U. Mosel, Phys. Rev. **C 60** (1999) 044614.
- [34] D. M. Manley and E. M. Saleski, Phys. Rev. **D 45** (1992) 4002.
- [35] B. Nilsson-Almqvist and E. Stenlund, Comp. Phys. Comm. **43** (1987) 387; B. Anderson, G. Gustafson and Hong Pi, Z. Phys. **C 57** (1993) 485.
- [36] K. Weber, B. Blättel, W. Cassing, H. C. Dönges, A. Lang, T. Maruyama and U. Mosel, Nucl. Phys. **A 552** (1993) 571.



- [37] S. Hama, B. C. Clark, E. D. Cooper, H. S. Sherif and R. L. Mercer, Phys. Rev. **C 41** (1990) 2737.
- [38] S. Teis, W. Cassing, M. Effenberger, A. Hombach, U. Mosel and Gy. Wolf, Z. Phys. **A 356** (1997) 421.
- [39] L. Ahle et al., Phys. Rev. **C 57** (1998) R466.
- [40] K. G. R. Doss et al., Phys. Rev. Lett. **57** (1987) 302.
- [41] H. Sorge, Phys. Rev. **C 52** (1995) 3291; Phys. Lett. **B 344** (1995) 35.
- [42] S. Voloshin and Y. Zhang, Z. Phys. **C 70** (1996) 665; A. M. Poskanzer and S. A. Voloshin, Phys. Rev. **C 58** (1998) 1671.

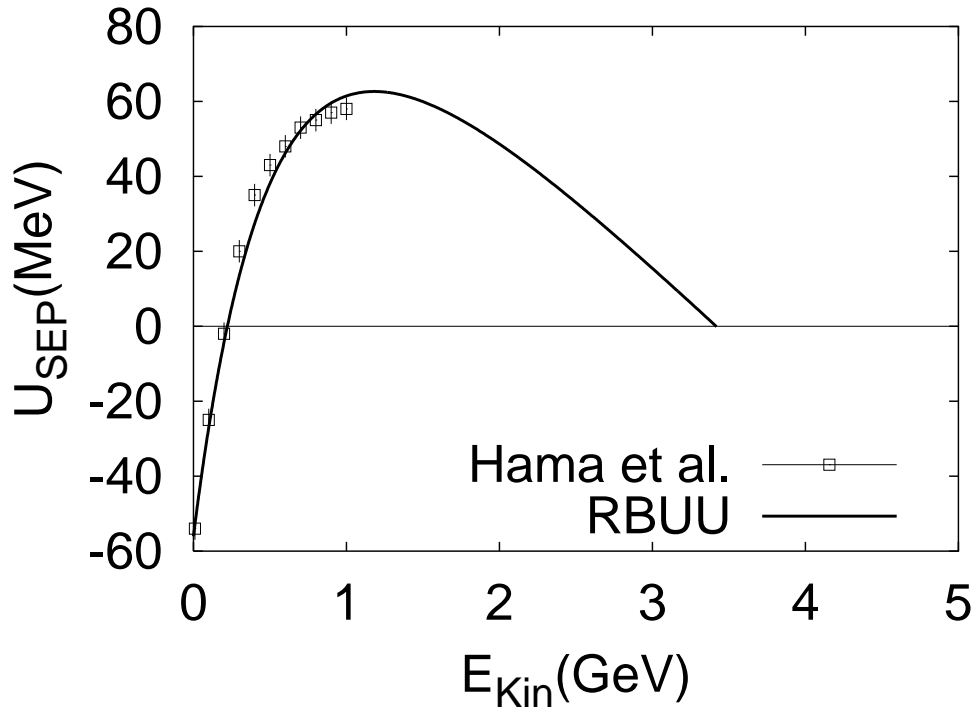


**Fig.1** The Schrödinger equivalent potential (2) at density  $\rho_0$  as a function of the nucleon kinetic energy  $E_{kin}$ . The solid curve (RBUU) results from the momentum-dependent potentials discussed in the text. The data points are from Hama et al. [37].

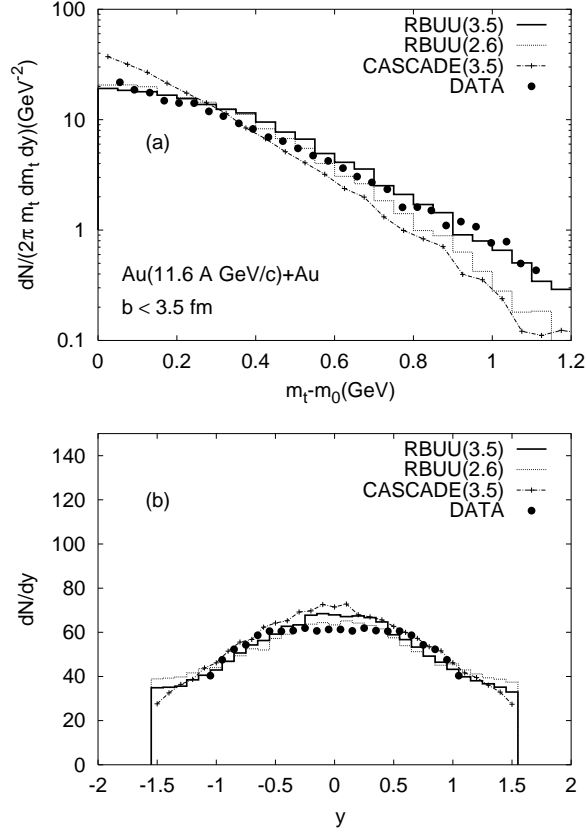


**Fig.2** (a) The transverse mass spectra of protons for Au + Au collisions at  $b < 3.5$  fm. The solid line and the dot-dashed line with crosses are results for  $\sqrt{s_{sw}}=3.5$  GeV with and without nuclear potentials, respectively. The dotted line RBUU(2.6 GeV) is for  $\sqrt{s_{sw}}=2.6$  GeV. The data points are taken from the E802 collaboration [39]. (b) Same as (a) but for the proton rapidity distribution.

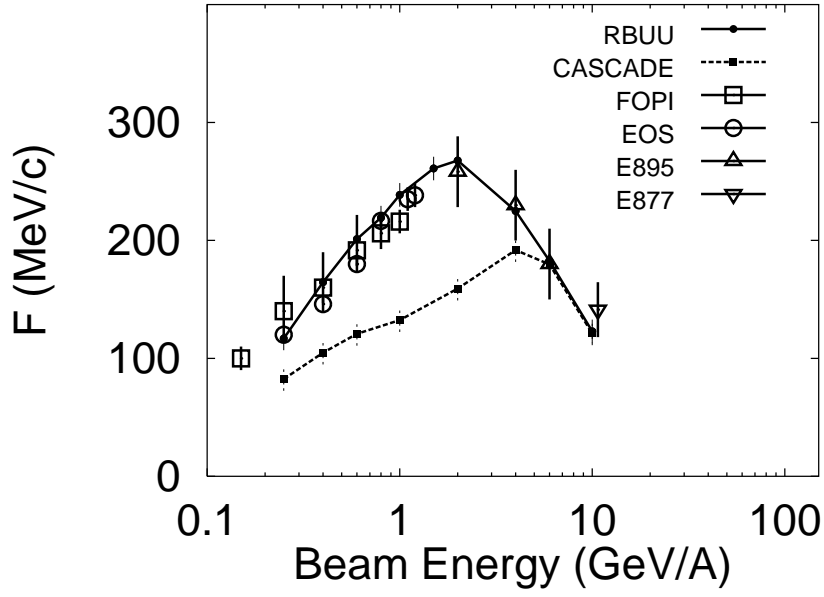


**Fig.3** The sideward flow  $F$  as a function of the beam energy per nucleon for Au + Au collisions at  $b = 6$  fm from the RBUU calculations. The solid line results for the parameter set RBUU, the dotted line for a cascade calculation with  $\sqrt{s_{sw}} = 3.5$  GeV. The data points are from the FOPI, EOS, E895 and E877 collaborations [7,9,13,16,17].

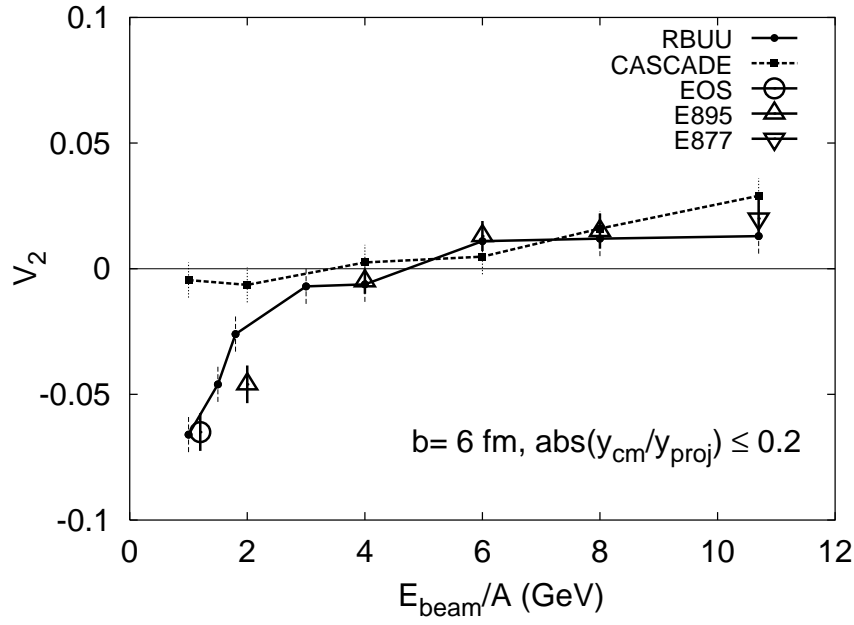


**Fig.4** The elliptic flow  $v_2$  of protons versus the beam energy per nucleon for Au + Au collisions at  $b = 6$  fm from the RBUU calculations. The solid line results for the parameter set RBUU, the dotted line for a cascade calculation with  $\sqrt{s_{sw}} = 3.5$  GeV. The data points are from the EOS, E895 and E877 collaborations [9,13,16,17].